Volume 256, number 1,2, 143–146 FEB 07687 October 1989

The structure of porin from *Rhodobacter capsulatus* at 0.6 nm resolution

M.S. Weiss*, T. Wacker, U. Nestel, D. Woitzik°, J. Weckesser°, W. Kreutz, W. Welte and G.E. Schulz*

**Institut für Organische Chemie und Biochemie, Institut für Biophysik und Strahlenbiologie, Albertstr. 23, D-7800 Freiburg i. Br.* and °*Institut für Biologie II, Mikrobiologie, Schänzlestr. 1, D-7800 Freiburg i. Br., FRG*

Received 14 August 1989

The crystal electron density map of porin from *Rhodobacter capsulatus* 37b4 at 0.6 nm resolution shows that the trimeric molecule consists of 3 merged cylinders as the central part, plus 3 laterally radiating domains. The density shows no prominent α-helices and is consistent with β-pleated sheet structure. The trimer density was dissected into monomers. Three separate pores per trimer with sizes that agree with the exclusion limit of permeating molecules could be identified. The cross-section of the central part as well as the pore distance agree with prior electron microscopy data on other porins.

Porin; Membrane protein structure; X-ray structure; (*Rhodobacter capsulatus*)

1. INTRODUCTION

Porins constitute the major class of integral membrane proteins in the outer membrane of gram-negative bacteria, where they form hydrophilic channels with some ion selectivity [1,2]. Polar molecules with M_r up to an exclusion limit of typically 600 can diffuse through these channels. The M_r of porins are in the range 30000–50000. Porins usually form trimers, they are very resistant to detergents and proteases. Porins contain predominantly β-sheet structures [3] in contrast to numerous other integral membrane proteins, a couple of which are structurally known [4–6]. Two-dimensional porin crystals have been studied by electron microscopy [7–10]. X-ray grade three-dimensional crystals were first reported by Garavito et al. [11]. We have recently obtained crystals of porin from *Rhodobacter capsulatus* 37b4 [12]. In contrast to other porins, that of *Rh. capsulatus* (and of closely related *Rh. sphaeroides* [13]) can be isolated under mild conditions as a monomer.

Correspondence address: M.S. Weiss, Institut für Organische Chemie und Biochemie, Albertstr. 21, D-7800 Freiburg i.Br., FRG

2. MATERIALS AND METHODS

Cultivation of *Rh. capsulatus* 37b4, preparation of porin and growing of crystals was carried out as described elsewhere [12]. For X-ray diffraction analysis the crystals were handled in a buffer containing 23% (w/v) PEG-600, 0.6% (w/v) *n*-octyltetraoxyethylene (C_8E_4), 10 mM EDTA, 300 mM LiCl, 3 mM NaN_3 and 20 mM Tris-HCl at pH 7.2. Crystals grew generally as regular, pointed rhombohedra with edge lengths up to 500 μm and edge angles of about 80°. They belong to space group R3. The homogeneity of porin before and after crystallization was checked by SDS-polyacrylamide-gel electrophoresis, which in both cases yielded two major bands at apparent M_r of 42000 and 43000. Moreover, the initial protein as well as a dissolved crystal gave the identical N-terminal amino acid sequences Glu-Val-Lys-Leu-Ser-Gly-Asp-Ala-.

For crystal screening we used precession photographs. Intensity data were collected at room temperature with a four circle diffractometer [14]. The native crystals diffract up to a resolution of 0.28 nm with mosaic spreads between 0.2° and 0.4°. Four native data sets were collected and averaged. Data quality was checked by internal R_F factors between 80 symmetry-related reflections [14], which were around 5% for native crystals as well as for derivatives. In contrast, the R_F values between the four full native sets were about 8%. This difference together with the variations of mosaic spread and cell

Published by Elsevier Science Publishers B.V. (Biomedical Division)
00145793/89/$3.50

Table 1

Heavy atom parameters for phasing[a]

Derivative[b]	R_F[c] (%)	Fractional coordinates			Occupancy (%)	F_H/E[d]
		x	y	z		
cis-Pt	28	0.038	0.140	0.000[e]	100	1.9
		0.981	0.720	0.993	83	
		0.856	0.061	0.243	57	
		0.219	0.334	0.036	34	
UO_2Ac_2	23	0.300	0.608	0.275	78	1.1
		0.485	0.304	0.273	68	
K_2PtCl_4	19	0.037	0.117	0.004	49	1.5
		0.995	0.727	0.002	80	
PIP	23	0.037	0.128	0.008	54	1.3
		0.986	0.721	0.000	82	
		0.150	0.413	0.000	20	

[a] The mean figure of merit was 0.68

[b] The abbreviated derivatives are *cis*-$Pt(NH_3)_2Cl_2$, uranylacetate, di-μ-iodobis(ethylenediamine)-diplatinum-nitrate (PIP). The soaking concentrations and times ranged from 1 to 5 mM and from 1 to 21 days

[c] R_F factor between native and derivative data sets [14]

[d] Phasing power, which is defined as root mean square heavy atom structure factor divided by the root mean square lack of closure error [15]

[e] Arbitrary definition of origin along the z-axis

parameters indicate that there exists some crystal packing heterogeneity.

For phasing we produced heavy atom derivatives by soaking and/or cocrystallizing with 41 heavy atom compounds. Visual comparison of precession photographs showed intensity changes in 10 derivatives, the data of which were then collected. Usually, derivatization had little effect on resolution and mosaic spread, while the radiation damage doubled. The difference Patterson map of the cis-Pt derivative (table 1) could be interpreted in terms of three sites. All other heavy atom positions were derived from difference Fourier maps. The heavy atom parameters were refined [15] and a 'best' electron density map [15] was calculated and interpreted.

3. RESULTS AND DISCUSSION

The diffractometer data of native crystals yielded the crystal axes a_{hex} = 9.53 nm (± 0.5%) and c_{hex} = 14.68 nm (± 0.2%), where the variations are significantly larger than the error of the measurements. The crystal density was 1.117 ± 0.007 g/ml as determined in gradients of bromobenzene and toluene. Taking into account the densities of the buffer (1.011 ± 0.004 g/ml), detergent (0.958 ± 0.012 g/ml) and protein (1.34 g/ml) and using a detergent : monomer molar ratio of 100 as found in crystals of OmpF [11], one derives that there is one porin monomer with M_r = 40000 ± 4000 in the asymmetric unit and that the crystal volume consists of 40% protein, 40% detergent C_8E_4 and 20% buffer.

The refinement data of the heavy atom derivatives are given in table 1 and the corresponding best electron density map is shown in the figures. The 16 z-sections depicted in fig.1 form a 4.4 nm layer and contain most of the trimeric molecule. Above and below these 16 sections, there are thinner extensions of the trimer along its (triad) axis, the total length is about 6.5 nm. The trimer consists of a central part of three merged cylinders with diameters of about 3.8 nm, plus three laterally radiating domains. The three merged cylinders centered at the lower right-hand triad can best be visualized in fig.1b; the lateral domains meet each other at the triad at the upper left-hand side. The cross-section of the merged cylinders agrees in shape and size with data from unstained porin PhoE of *E. coli* as derived from electron diffraction studies [10].

Within the 4.4 nm layer depicted in fig.1, the trimers form a trigonal array with a distance of 9.53 nm defined by the contact between lateral domains. The three triads are at the molecular axis, at the contact between lateral domains and in a spacious solvent region (not shown in fig.1). This lateral arrangement is likely to correspond to the packing in the membrane. This notion is corroborated by the observation of a very similar lattice with a trimer–trimer distance of 9.2 nm in the stalks of a thermophilic bacterium that are built up mainly by porin [9]. Note that the in vivo array in the stalk requires a lateral spacer if the diameter of the central part of this porin is about 6.5 nm as in the porin reported here and in PhoE [13]. In the crystal, successive layers stack onto each other with the trimers in rhombohedral packing, so that each of the three crystallographic triads accommodates a molecular triad in due turn. The contacts along the c-axis are between heads and tails of the central parts of the trimers, which have a small overlap in the z-projection. These contacts are probably polar and suffice to form the three-dimensional lattice. The observed larger and smaller variations of the a- and c-axes of the native crystals, respectively, correspond to the

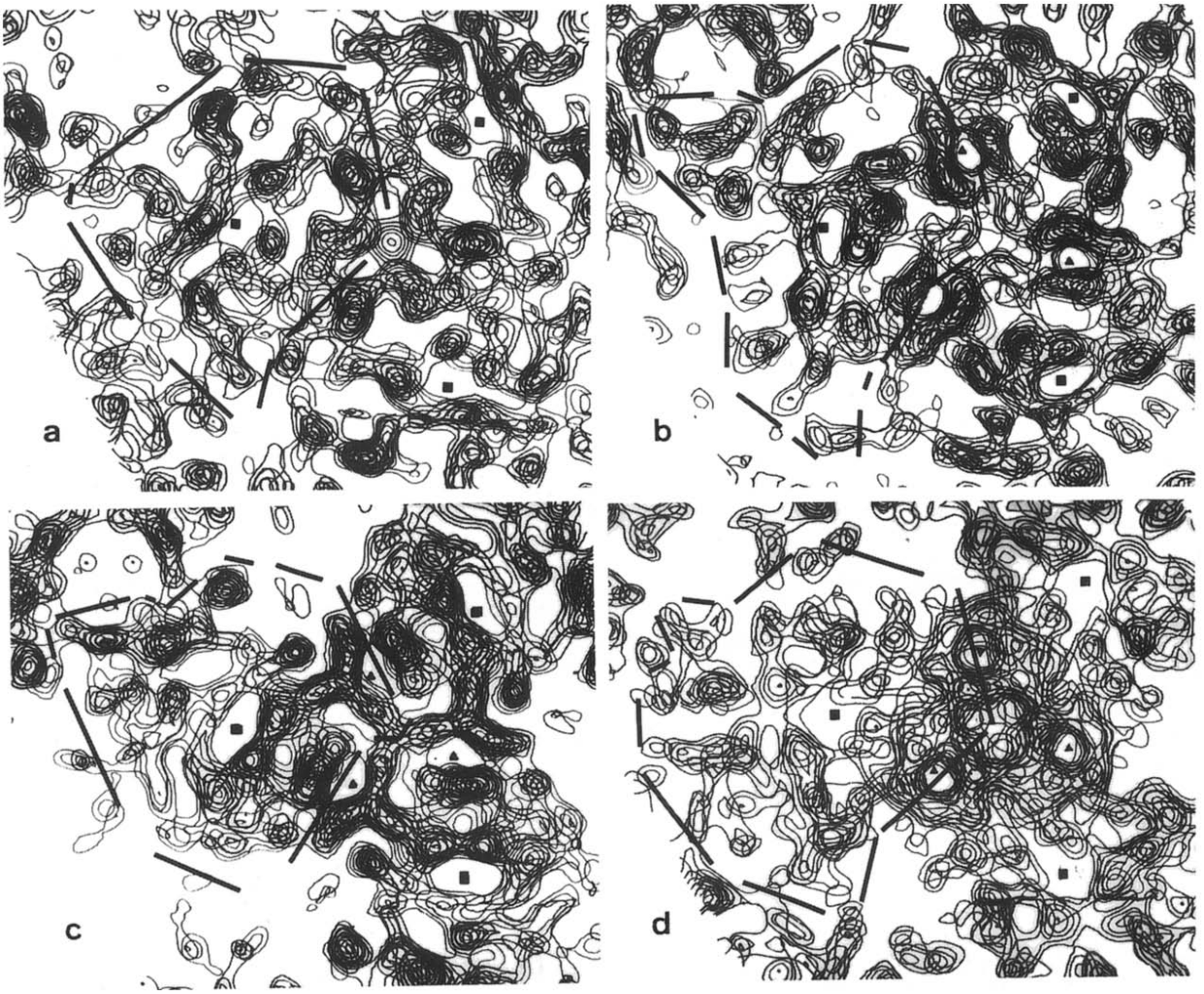

Fig.1. Multiple isomorphous replacement map of porin from *Rhodobacter capsulatus* 37b4 at 0.6 nm resolution. Depicted are the *z*-sections 7/54 through 22/54 at density levels 12, 24, ...96% of maximum. The distance between the triads at the upper left-hand and the lower right-hand sides is 5.5 nm. The best solution for the boundary of a monomer is marked. The channels at mutual distances of 2.1 nm and 4.7 nm are marked by (▲) and (■), respectively. Each picture contains four *z*-sections which span 1.1 nm. (*a*) Sections 7/54 to 10/54, (*b*) sections 11/54 to 14/54, (*c*) sections 15/54 to 18/54, (*d*) sections 19/54 to 22/54.

presumably better defined longitudinal (along *z*) than transversal (along *x*) components of these contacts. They indicate further that the *intra*-membrane contacts between the lateral domains are not as rigid as those between the central parts.

In the map, the trimer and individual lateral domains could be outlined easily. Less obvious, however, was the subdivision of the three merged cylinders into monomers. The best interpretation is marked in fig.1; it necessitates cuts through density near the triad. No prominent α-helices can be found in the map. The density shapes are consistent with β-pleated sheet structures and thus with spectroscopic data [3]. The electron density is rather peculiar as it contains a number of encapsulated low-density regions. Most spectacular is the *z*-section 17/54 shown in fig.2, which is included in fig.1c. The occurrence of so many cavities is not at all common for water-soluble proteins. Presumably, they contain sequestered water. A porous structure was also indicated when the monomer size was derived from the map by outlin-

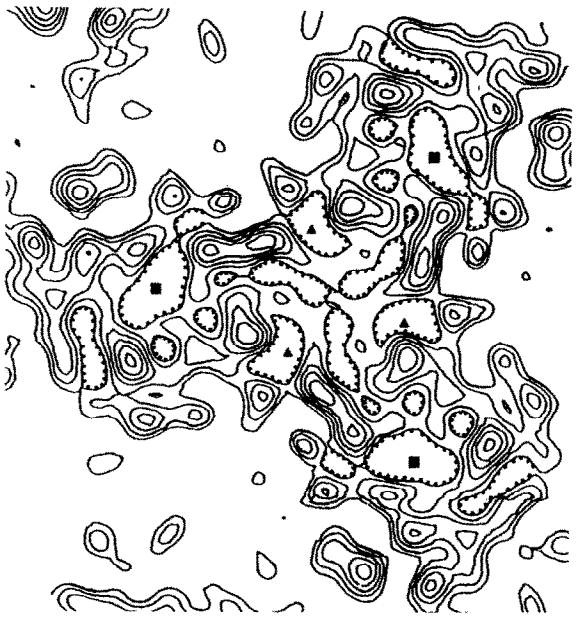

Fig.2. Section 17/54 of fig.1 singled out. All speckled enclosed areas contain densities below the first level. Such cavities are very rare in 0.6 nm maps of water-soluble proteins. The large number observed here is quite noticeable.

ing the surface and measuring the internal volume. Only by assigning large (≥0.6 nm diameter) cavities as 'outside' we arrived at an M_r corresponding to the gel electrophoresis data and to the M_r of other porins, while the inclusion of cavities increased M_r to the 60000 range. An internal volume comparison between the central part and the lateral domains indicates an M_r of about 10000 for a lateral domain.

In order to identify the pores, we looked for cavities that run along z and span the merged cylinders. In our map, there is no transversing pore at the molecular triad or at the center of an individual cylinder; both regions are clearly blocked (fig.1). There exists a narrow channel at the interface of the best monomer outline (fig.1), which is surrounded by strong density along its whole path and has an *inter*-channel distance of 2.1 nm within a trimer. But the channel diameter is only 0.5 nm or less, which contradicts the exclusion limit for permeating molecules [16]. A larger channel with a cross-section of 0.6 nm by 1.0 nm, which would allow the permeation of molecules up to an M_r of about 600, transverses each monomer further away from the molecular triad with an *inter*-channel distance of 4.7 nm. It is most likely the main pore (fig.1).

Our results can be related to electron microscopy studies on other porins. A three-dimensional map of negatively stained PhoE shows three stain-filled channels [10], the bulk of which are at a mutual distance of 4.5 nm. This distance agrees well with our pore assignment and rules out the narrow channels with a mutual distance of 2.1 nm. A three-dimensional map of negatively stained porin OmpF of *E. coli* showed three stain-filled channels [8] with a mutual distance of 4.5 nm which corresponds also to our pore assignment. Similar data have been obtained from a thermophilic bacterium [9]. It should be noted that the stain-filled channels in OmpF merge at one side [8] and come closer together at one side in PhoE [10]. These observations could be explained by stain merging at one of the trimer ends or by stain penetration into the presumably porous inside of the trimer.

REFERENCES

[1] Nikaido, H. and Vaara, M. (1985) Microbiol. Rev. 49, 1–32.
[2] Benz, R. and Bauer, K. (1988) Eur. J. Biochem. 176, 1–19.
[3] Nabedryk, E., Garavito, R.M. and Breton, J. (1988) Biophys. J. 53, 671–676.
[4] Henderson, R. and Unwin, P.N.T. (1975) Nature 275, 28–32.
[5] Deisenhofer, J., Epp, O., Miki, K., Huber, R. and Michel, H. (1985) Nature 318, 618–624.
[6] Feher, G., Allen, J.P., Okamura, M.Y. and Rees, D.C. (1989) Nature 339, 111–116.
[7] Chang, C.-F., Mizushima, S. and Glaeser, R.M. (1985) Biophys. J. 47, 629–639.
[8] Engel, A., Massalski, A., Schindler, H., Dorset, D.L. and Rosenbusch, J.P. (1985) Nature 317, 643–645.
[9] Chalcroft, J.P., Engelhardt, H. and Baumeister, W. (1987) FEBS Lett. 211, 53–58.
[10] Jap, B.K. (1989) J. Mol. Biol. 205, 405–419.
[11] Garavito, R.M., Jenkins, J., Jansonius, J.N., Karlsson, R. and Rosenbusch, J.P. (1983) J. Mol. Biol. 164, 313–327.
[12] Nestel, U., Wacker, T., Woitzik, D., Weckesser, J., Kreutz, W. and Welte, W. (1989) FEBS Lett. 242, 405–408.
[13] Weckesser, J., Zalman, L.S. and Nikaido, H. (1984) J. Bacteriol. 159, 199–205.
[14] Thieme, R., Pai, E.F., Schirmer, R.H. and Schulz, G.E. (1981) J. Mol. Biol. 152, 763–782.
[15] Dickerson, R.E., Weinzierl, J.E. and Palmer, R.A. (1968) Acta Crystallogr. B24, 997–1003.
[16] Flammann, H.T. and Weckesser, J. (1984) J. Bacteriol. 159, 410–412.